tary condition applies,[3]

$$S\tilde{S}^* = 1, \tag{2}$$

where $\tilde{S}^*$ is the conjugate transpose matrix. Considering the off-diagonal element of (2),

$$s_{12}s_{32}^* + s_{14}s_{34}^* = 0 \tag{3}$$

or

$$\theta_{12} - \theta_{32} = \pi + \theta_{14} - \theta_{34}, \tag{4}$$

where θ_{12}, θ_{32}, θ_{14} and θ_{34} are the argument of s_{12}, s_{32}, s_{14} and s_{34}, respectively. From the principal diagonal element of (2),

$$s_{12}s_{12}^* + s_{14}s_{14}^* = 1 \tag{5}$$

or

$$|s_{12}|^2 + |s_{14}|^2 = 1. \tag{6}$$

By choosing the location of the reference planes

$$\theta_{14} = \theta_{32} = 0, \tag{7}$$

(4) becomes

$$\theta_{12} + \theta_{34} = \pi. \tag{8}$$

A loop-type coupler, with the coupling loop placed near the side wall of the waveguide, is shown in Fig. 2. This device was tested for 15 kw average and 10 Mw peak. The coupling variation over the full waveguide frequency range is shown in Fig. 3. This figure shows the coupling with the loop at the center of the waveguide and near the side wall. The increase in coupling value as a function of coupling-loop position is

$$C = 20 \log \left(\frac{1}{\cos \pi d} \right), \tag{9}$$

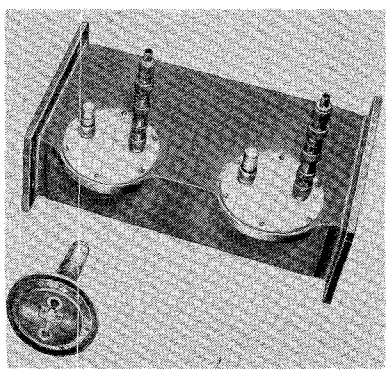

Fig. 2—Loop-type coupler.

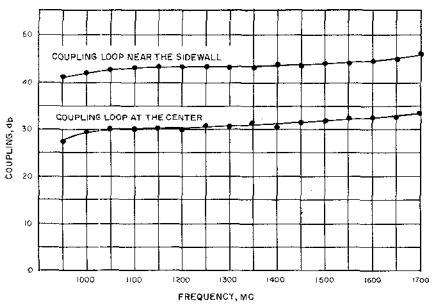

Fig. 3—Characteristics of loop-type coupler with coupling loop at the center and near the side wall.

[3] C. G. Montgomery, R. H. Dicke and E. M Purcell, "Principles of Microwave Circuits," McGraw-Hill Book Co., Inc., New York, N. Y., pp. 301–303; 1948.

where d is the displacement in fractions of the a dimension of the guide, and is measured from the center of the guide toward the side wall. The experimental and calculated values of this variation are shown in Fig. 4. Measurements were made at two frequencies differing by 10 Mc. The results show that the variation in coupling is frequency insensitive as indicated by (9). A minimum directivity of 30 db was achieved over 10 per cent of the band by adjusting the location, height and length of the rectangular-shaped plate situated around the coupling loop and grounded to the top wall of the waveguide. Fig. 5 indicates the change in directivity as a function of frequency. It is felt that a directivity greater than 40 db exists at the center frequency. This value could not be measured due to the lack of proper termination. A 50-Ω coaxial termination with VSWR of less than 1.03 was utilized with the auxiliary arm of the coupler.

ACKNOWLEDGMENT

The author would like to acknowledge many helpful discussions with S. Ammirati, who proposed the use of the hood over the coupling loop to increase the directivity, and with S. Lehr. He is also indebted to J. Ebert for his many helpful suggestions.

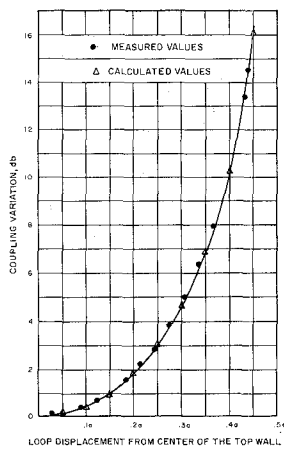

Fig. 4—Coupling variation as a function of loop position.

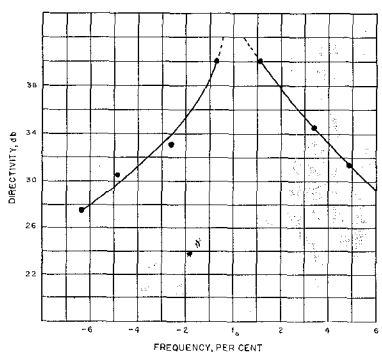

Fig. 5—Directivity vs frequency.

B. MAHER
Microwave Div.
FXR, Inc.
Woodside, N. Y.

The Cutoff Wavelengths of Composite Waveguides*

When electromagnetic waves propagate in waveguides of nonsimple cross section, no exact solution can be obtained by the conventional method of solving the wave equation by separation of variables. In such cases approximations are available such as perturbation methods, variational methods, etc.[1]

The Rayleigh-Ritz method has been used to obtain an approximate solution for the cutoff wavelength for waveguides with semicircular side walls and flat top and bottom walls, and for truncated-circular waveguides. See Figs. 1 and 2.

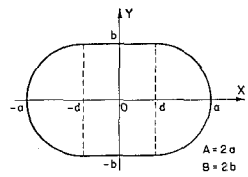

Fig. 1—Waveguide with flat tops and bottoms and semicircular side walls.

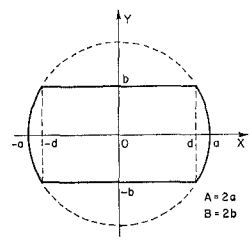

Fig. 2—Truncated-circular waveguide.

The results obtained for the cutoff wavelengths for waveguides of semicircular side walls and flat top and bottom walls disagree with the values shown by Montgomery, Dicke and Purcell[2] for aspect ratios of 0.406 and 0.450. From the nature of the problem and from experimental evidence it can be stated that the trial functions used to obtain the results[2] mentioned above was inferior to the one used here.

The boundary-value problem of electromagnetic waves propagating in a cylindrical waveguide can always be reduced to a simple two-dimensional problem.

If the longitudinal axis is in the z direction,

$$\nabla^2\psi_i(x, y) + k_i^2\psi_i(x, y) = 0, \tag{1}$$

where $\psi_i(x, y)$ is the eigenfunction and k_i is the propagation constant for the ith mode, respectively.

If ψ_i satisfies either Dirichlet or Neumann boundary conditions, a variational expression for the eigenvalue k_i^2 exists,

$$k_i^2 \leq \frac{\int |\nabla\psi_i|^2 d\sigma}{\int \psi_i^2 d\sigma} \tag{2}$$

* Received by the PGMTT, March 14, 1961; revised manuscript received, April 17, 1961.

[1] P. M. Morse and H. Feshbach, "Methods in Theoretical Physics II," McGraw-Hill Book Co., Inc., New York, N. Y.; 1953.

[2] C. G. Montgomery, R. H. Dicke and E. M. Purcell, "Principles of Microwave Circuits," M.I.T. Rad. Lab. Ser., McGraw-Hill Book Co., New York, N. Y., vol. 8, p. 45; 1948.

the integrals taken over the waveguide cross section.

Following the work of Kornhauser,[3] a trial function can be used to obtain an approximate value for the eigenvalue for the fundamental mode.[4]

Dropping subscripts, a legitimate trial function for the fundamental mode is

$$\psi(x) = \sum_{n=0}^{N} C_{2n+1}x^{2n+1}. \qquad 3)$$

Note that the trial function does not satisfy the boundary condition, also that the parameters C_{2n+1} will be adjusted to minimize the eigenvalue.

Let $N=1$; then

$$\psi = C_1x + C_3x^3. \qquad (4)$$

By inserting the trial function in (2), the eigenvalue takes the following form:

$$k^2 = \frac{\alpha C_1^2 + \beta C_1C_3 + \gamma C_3^2}{\delta C_1^2 + \epsilon C_1C_3 + \zeta C_3^2}, \qquad (5)$$

where $\alpha, \beta, \gamma, \delta, \epsilon$ and ζ are constants dependent on the dimensions of the waveguide.

The eigenvalue k^2 is next minimized with respect to C_1 and C_3. After eliminating C_1 and C_3, k^2 is obtained from

$$k^4 - 2\Theta k^2 + \Phi = 0, \qquad (6)$$

where

$$\Theta = \frac{2\alpha\zeta + 2\delta\gamma - \epsilon\beta}{4\delta\zeta - \epsilon^2}$$

$$\Phi = \frac{4\alpha\gamma - \beta^2}{4\delta\zeta - \epsilon^2}.$$

For the waveguide of semicircular side walls and flat top and bottom walls, the coefficients are

$$\alpha = a\left[p + \frac{\pi}{4}r\right]$$

$$\beta = a^3\left[2p^3 + \frac{3\pi}{2}p^2r + 4pr^2 + \frac{3\pi}{8}r^3\right]$$

$$\gamma = a^5\left[\frac{9}{5}p^5 + \frac{9\pi}{4}p^4r + 12p^3r^2 + \frac{27\pi}{8}p^2r^3 + \frac{24}{5}pr^4 + \frac{9\pi}{32}r^5\right]$$

$$\delta = a^3\left[\frac{1}{3}p^3 + \frac{\pi}{4}p^2r + \frac{2}{3}pr^2 + \frac{\pi}{16}r^3\right]$$

$$\epsilon = a^5\left[\frac{2}{5}p^5 + \frac{\pi}{2}p^4r + \frac{8}{3}p^3r^2 + \frac{3\pi}{4}p^2r^3 + \frac{16}{15}pr^4 + \frac{\pi}{16}r^5\right]$$

$$\zeta = a^7\left[\frac{1}{7}p^7 + \frac{\pi}{4}p^6r + 2p^5r^2 + \frac{15\pi}{16}p^4r^3 + \frac{8}{3}p^3r^4 + \frac{15\pi}{32}p^2r^5 + \frac{48}{105}pr^6 + \frac{5\pi}{256}r^7\right],$$

where $r=b/a$ and $p=1-r$.

[3] E. T. Kornhauser and I. Stakgold, "Application of Variational Methods to the Equation $\nabla^2u+\lambda u=0$," Cruft Lab., Harvard Univ., Cambridge, Mass., Tech Rept. No. 117; 1950.

[4] The fundamental mode is the equivalent to the H_{10} mode in rectangular waveguide and the H_{11} mode in circular waveguide

The numerical results, the experimental points and the points obtained from Montgomery, Dicke and Purcell[2] are shown in Fig. 3.

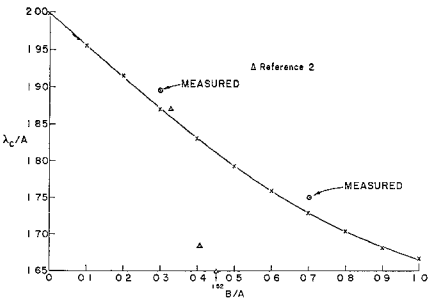

Fig. 3—The cutoff wavelengths for the waveguide with flat tops and bottoms and semicircular waveguides as a function of aspect ratio.

The method has also been applied to calculate the cutoff wavelengths for truncated-circular waveguides.[5]

G. R. Valenzuela
The Johns Hopkins University
Radiation Lab.
Baltimore, Md.

[5] G. R. Valenzuela, "The Cut-Off Wavelengths and Power-Voltage Impedance for Composite Waveguides for the Fundamental Mode," Rad. Lab., The Johns Hopkins Univ., Baltimore, Md., Tech. Rept., to be published.

A Mechanical Waveguide Hybrid Phase Shifter*

Some interesting results have been obtained on a waveguide-hybrid phase shifter under development for use in an *S*-band radio-astronomy interferometer antenna.

The phase shifter[1,2] illustrated in Fig. 1(a) comprises a waveguide hybrid junction, a rotating chopper, and a pair of variable lengths of a short-circuited waveguide: the variable lengths of the guide are provided by a movable short-circuit plunger. The operation of the phase shifter is as follows.

Let us assume that the chopper is initially closed. When power is injected at port 1, the power enters the hybrid junction where it is divided, one half being coupled to the adjacent waveguide where it continues to propagate in the same direction, while the other half of the power propagates in the main waveguide. The properties of the hybrid junction are such that the signal in the adjacent waveguide is in phase quadrature, lagging the signal in the main waveguide. At the chopper the two signals are reflected; power in the main waveguide enters the hybrid junction, recombining in phase with the power in the adjacent arm. The entire power leaves port 2, provided that the hybrid is matched. If, now, the chopper is opened, an additional path length is introduced into the hybrid system and the amount of phase shift is equivalent to an electrical length of twice the stub length. The phase shift can be made to be proportional to either the stub length s or to $(\lambda_g/2)-s$, where λ_g is the guide wavelength, depending upon how the chopper is introduced across the waveguide.

A sketch of the chopper used in the model under investigation is shown in Fig. 1(b). In the radio-astronomy application the chopper rotates at a speed of 900 rpm. The phase-shift characteristics as a function of chopper rotation are shown in Fig. 2 for two different plunger positions. Note particularly that the shorter stub length provides the greater amount of phase shift. For this case the phase shift is proportional to $(\lambda_g/2)-s$. This result can be explained quite readily if one analyzes the behavior of the chopper and stub in terms of an equivalent circuit.

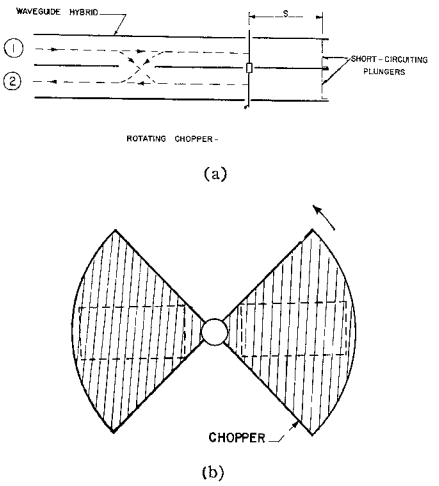

Fig. 1(a) Waveguide hybrid phase shifter. (b) Rotating chopper used in the phase shifter.

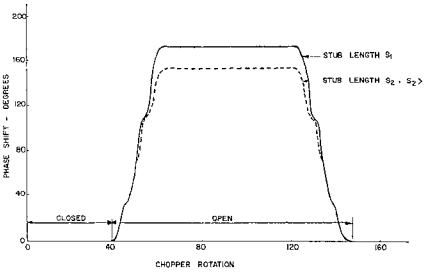

Fig. 2—Phase-shift characteristics as a function of chopper rotation.

The susceptance of the short-circuited stub is plotted as a point Y_{s1} on the Smith Chart diagram shown in Fig. 3 Placed in shunt with Y_{s1} is the susceptance of the chopper which behaves as a capacitive iris (positive susceptance). As the chopper is introduced, the net susceptance is reduced,

* Received by the PGMTT, April 17, 1961.

[1] H. Shnitkin, "Survey of electronically scanned antennas," *Microwave J.*, vol. 4, pp. 57–64; January, 1961.

[2] J. Blass, *et al.*, "A High Speed *X*-Band Conical Scanner," AF Cambridge Res. Ctr., Bedford, Mass., AFCRC Rept. TR-58-145-11; April, 1958.